Formation of epitaxial β -Sn islands at the interface of SiO 2∕Si layers implanted with Sn ions

J. M. J. Lopes, F. C. Zawislak, P. F. P. Fichtner, R. M. Papaléo, F. C. Lovey, A. M. Condó, and A. J. Tolley

Citation: Applied Physics Letters **86**, 191914 (2005); doi: 10.1063/1.1927710
View online: http://dx.doi.org/10.1063/1.1927710
View Table of Contents: http://scitation.aip.org/content/aip/journal/apl/86/19?ver=pdfcov
Published by the AIP Publishing

Formation of epitaxial β-Sn islands at the interface of SiO_2/Si layers implanted with Sn ions

J. M. J. Lopes and F. C. Zawislak
Instituto de Física–UFRGS, 91501-970 Porto Alegre, Brazil

P. F. P. Fichtner[a)]
Departamento de Metalurgia, Escola de Engenharia - UFRGS, Porto Alegre, Brazil

R. M. Papaléo
Faculdade de Física, Pontificia Universidade Católica (PUC-RS), Porto Alegre, Brazil

F. C. Lovey, A. M. Condó,[b)] and A. J. Tolley[b)]
Centro Atómico Bariloche, 8400 S. C. Bariloche, Argentina

(Received 3 December 2004; accepted 29 March 2005; published online 5 May 2005)

180 nm SiO_2 layers on Si (100) were implanted with Sn ions producing a profile with a peak concentration of 3 at. % at the middle of the oxide. After high temperature (900–1100 °C) annealing, an array of β-Sn islands epitaxially attached to the Si was observed at the SiO_2/Si(100) interface due to the migration of the implanted Sn atoms. The breakdown of the planar SiO_2/Si interface and the appearance of the island system is discussed in terms of the Sn–Si equilibrium properties. Our results reveal a new method to create a high density of nanosized islands with good uniformity in size and shape. © *2005 American Institute of Physics*. [DOI: 10.1063/1.1927710]

The implantation of Sn ions into SiO_2/Si films has been studied in connection with the formation of nanostructures exhibiting intense visible and ultraviolet photoluminescence (PL). The PL was associated to oxygen deficiency centers created during the implantation and annealing processes,[1,2] very probably assisted by the development of the nanoparticle system.[3] In addition, the formation of a rather dense array of Sn rich nanoparticles presenting a narrow size dispersion and located within the oxide but very close to the SiO_2/Si interface has been observed and considered of potential interest for flash memory applications.[4] This peculiar microstructure evolution behavior has been explained in terms of collision damage caused by the ions or the oxide atom recoils at the interface.[5] More recently, it has been shown that the annealing atmosphere also influences the microstructure development of Sn^+ implanted silica layers,[6,7] with significant effects in blue-violet PL response.[7]

This letter demonstrates an additional aspect of the microstructure evolution of the Sn^+ implanted silica layers. In particular, we report on the formation of a rather dense array of nanosized epitaxial β-Sn islands presenting flat tops and rather steep edges at the interface of SiO_2/Si(100) layers. Our method contrasts with those based on layer-by-layer deposition methods on free surfaces, which require a rigorous control of surface contamination and ultrahigh vacuum conditions. The formation of the β-Sn islands is discussed in terms of the solubility and diffusivity of the Sn–Si system.

SiO_2 films 180 nm thick were thermally grown on crystalline Si (100) substrates in a dry ambient at 1000 °C. These films were implanted at room temperature with 200 keV Sn ions to a fluence of 1.5×10^{16} cm^{-2}, producing a Gaussian-like Sn concentration-depth profile with a peak concentration of ≈3 at. % at a depth of ≈90 nm from the surface. Postimplantation thermal annealings were performed in the 900–1100 °C temperature range by conventional furnace processing in dry N_2 ambient for 30 min. The concentration-depth distribution profiles of the Sn atoms were determined by Rutherford backscattering spectrometry (RBS) and the obtained nanostructures were investigated by transmission electron microscopy (TEM) using cross-section and plan-view samples prepared by ion milling. The plan-view samples were also chemically thinned to reduce the oxide thickness, allowing a better observation of the SiO_2/Si(100) interface region.

Figure 1 shows the thermal evolution of the Sn concentration-depth profile in the implanted samples, as given by RBS measurements. With increasing temperature, the Sn profile redistributes and, for 1000 and 1100 °C, a conspicuous accumulation of about 20% and 35% of the total

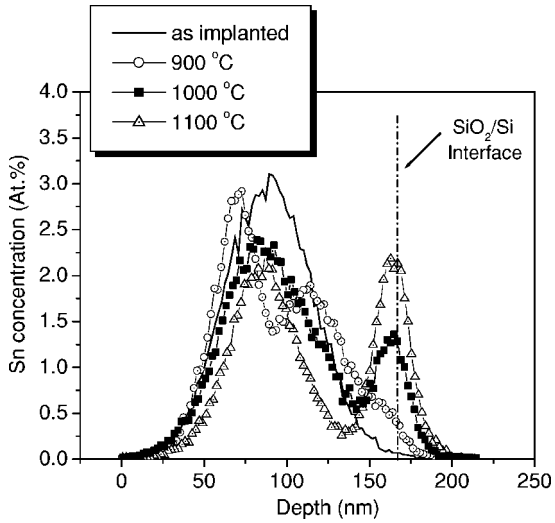

FIG. 1. Sn concentration-depth profiles obtained by RBS for the as-implanted and annealed (900, 1000, and 1100 °C) samples.

[a)]Author to whom all correspondence should be addressed; electronic mail: fichtner@if.ufrgs.br
[b)]Also at: CONICET, Argentina.

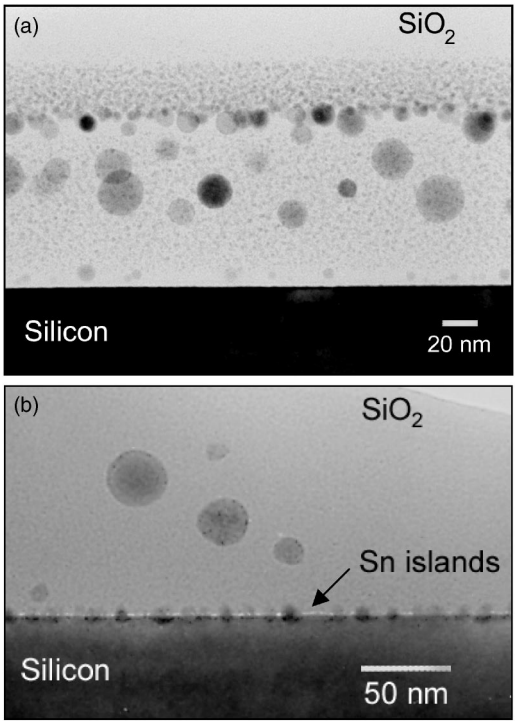

FIG. 2. Cross-sectional TEM images showing the Sn nanoclusters within the SiO_2 layer after annealing at 900 °C (a) and 1100 °C (b).

Sn content takes place at the SiO_2/Si interface, respectively. The Sn atoms remaining inside the SiO_2 film are associated with the presence of nanoparticles (Fig. 2). After annealing at 900 °C [Fig. 2(a)], the co-existence of two systems of nanoparticles is observed. The first one consists of large particles (mean diameter around 20 nm) presenting a crystalline Sn-rich core and a poly-crystalline halo containing SnO_x nanoparticles.[7] The second system is composed of a denser array of nanoparticles with typical diameters from 2 to 4 nm. At 1100 °C [Fig. 2(b)], the larger particles have further coarsened and are the only ones present inside the film. Moreover, a dense array of acute structures is clearly observed at the SiO_2/Si interface as shown in Fig. 2(b). These structures show a strain-induced contrast within the Si substrate suggesting the buildup of a misfit-induced strain field.

Details of the interface nanostructures are shown in Fig. 3. It shows cross-section high-resolution TEM images of islands formed upon annealing at 1000 °C [Figs. 3(a) and 3(b)], and at 1100 °C [Figs. 3(c) and 3(d)]. The lattice images were obtained with the substrate aligned along the [011] axis parallel to the (100) surface plane. They show epitaxial islands emerging from the Si substrate. The insets in these figures are fast-Fourier-transform (FFT) patterns of the island images. These patterns are well fitted by simulations which assume a β-Sn structure[8] and the corresponding Miller indices are given in Fig. 3. Particles with several different orientations relative to the silicon substrate were observed. Figures 3(a) and 3(c) give examples of particles with the $[100]_\beta$ zone axis parallel to the electron beam. In these particles, the $[023]_\beta$ axis is closely parallel to the $[100]_{Si}$ one. Figures 3(b) and 3(d) show particles with a different orientation relationship with the substrate. The FFT patterns of these particles are consistent with either $[101]_\beta$ or $[001]_\beta$ zone axes.

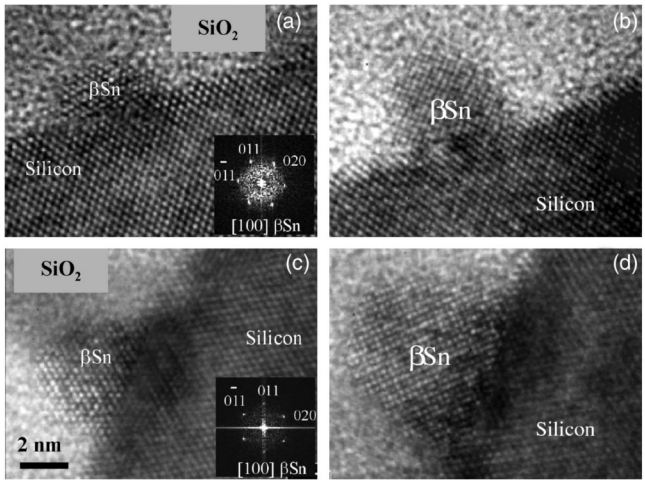

FIG. 3. High-resolution TEM images of islands formed upon annealing at (a) and (b) 1000 °C and (c) and (d) 1100 °C. The insets in (a) and (c) present fast-Fourier-transform patterns from the island images.

Figure 4(a) shows a plan-view TEM micrograph for the sample annealed at 1100 °C, obtained under diffraction contrast imaging conditions close the [100] axis of the silicon matrix. The combination of these observations with the cross-sectional images reveals that the island dimensions evolve with the annealing temperature and thus with the Sn content at the SiO_2/Si interfacial region (see Fig. 1). Although for 1000 °C the interface protuberances present a typical height of 2.5 nm with a 4 nm base, the treatment at 1100 °C leads to the growth of an array of higher islands (3–4 nm high) showing a near square-like basis with mean size of 6.2 ± 0.8 nm. Their area concentration is $\approx 6.6 \times 10^{11}$ cm^{-2} and the center-to-center mean distance between first-neighbor islands is 15 ± 3.5 nm.

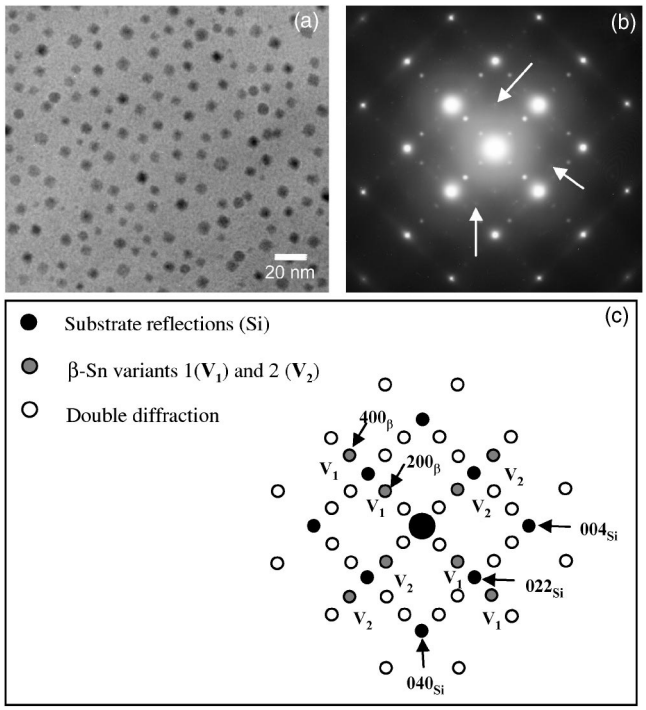

FIG. 4. Plan-view TEM micrograph, for the sample annealed at 1100 °C, (a) under structure factor imaging conditions along the [100] axis of the silicon substrate; (b) selected area diffraction (SAD) pattern from the plan-view observations; and (c) key diagram of the diffraction pattern.

Figure 4(b) shows the selected area diffraction pattern from the plan-view observations shown in Fig. 4(a). The strong reflections are from the [100] zone axis of the Si matrix and the weak reflections are from the islands. They are indexed in the key diagram in Fig. 4(c). The most intense β-Sn reflections arise from islands of the type shown in Figs. 3(a) and 3(c). There are two variants of such orientation relationship arranged at 90° to each other [labeled V_1 and V_2 in Fig. 4(c)]. The most prominent reflections from particles with the orientation relationship shown in Fig. 3(b) are coincident with those of the Si substrate. In addition, other very weak reflections in Fig. 4(b) can be observed (indicated with arrows). The interplanar distances of such reflections are also consistent with the β-Sn structure, indicating that particles with other orientation relationships to the substrate are present. Lattice images of such particles have also been observed in the cross section specimens.

The equilibrium properties of the Sn–Si system can provide a simple explanation for the formation of the observed β-Sn islands. The Sn–Si equilibrium phase diagram[9] shows a solid-solution field of Sn in Si where the maximum Sn concentration continuously increases with the temperature, corresponding to 0.065 at. % at 900 °C and achieving a maximum value of $\approx$0.1 at. % at 1065 °C. The phase diagram also presents an eutectic point with $T_e \approx 232$ °C, very close to the pure Sn side. Hence, during annealing at temperatures between 900 and 1100 °C, the formation of a Sn solid solution in the Si matrix may take place and therefore the interface becomes a sink for Sn atoms from the oxide film. As a consequence, a diffusion-controlled Sn redistribution toward the interface is expected, as is in fact observed by the RBS measurements (see Fig. 1). During subsequent cooling of the sample, the Sn atoms in solution start to segregate at the interface as their solubility limit decreases with the temperature. Since interfaces provide a rather high diffusivity path, Sn agglomeration should be favored, but large Sn droplets have not been observed. Probably a large agglomeration of Sn has been prevented by the formation of extended Sn rich melt-like zones with rather low interface energy (i.e., high wettability). When the eutectic temperature is reached, Sn solidifies causing the formation of a large number of small and coherent Sn islands.

The diffusive growth and ripening of the island system seems to be dependent on the Sn content segregated at the SiO_2/Si interface. The increasing of the annealing temperature leads to a higher amount of Sn available at the interface and consequently to the coarsening of larger islands in order to minimize the interface energy of the system within the kinetic constrains of the Sn diffusion length at the eutectic temperature. In contrast, for longer annealing times, it is expected that the Sn solid solution should be more uniform and extend to a larger depth inside the Si matrix. Hence, during the cooling stage, the segregation of Sn toward the interface may compete with a phase separation process, very probably driven by a transient stage of spinodal decomposition. In fact, for samples annealed during 180 min at 1100 °C, preliminary results show the suppression of the island system and the appearance of Sn-rich nanoparticles embedded in the Si matrix close to the SiO_2/Si interface, which may be related to the spinodal process. The formation of such Sn_xSi_{1-x} islands may offer the possibility to obtain direct band gap semiconducting nanostructures.[10]

In summary, it was demonstrated that, upon Sn ion implantation and subsequent annealing, a high density of Sn epitaxial islands with β-Sn structure can be formed at the $SiO_2/Si(100)$ interface. This island system presents good uniformity in size and shape and a narrow distribution of distances between first-neighbor islands. The formation process of the islands may be thermally controlled according to the equilibrium properties of the Sn–Si system. This new method to form nanosized Sn islands may also be extended to other elements with similar equilibrium properties with respect to Si. For instance, the island growth of compound semiconductors such as PbS or PbSe via co-implantation in SiO_2/Si layers is very promising due to the interesting quantum confinement properties of these materials,[11,12] with potential applications in future Si-based optoelectronic devices.

This work was partially supported by the Brazilian agencies CNPq, CAPES, and FINEP. One of the authors (P.F.P.F.) also thanks the support from the Alexander von Humboldt Foundation, Germany, and two of the authors (A.M.C. and A.J.T.) thank the support from CONICET, Argentina. The authors would also like to acknowledge the help of T. L. Marcondes in the TEM sample preparation.

[1] L. Rebohle, J. von Borany, H. Frob, and W. Skorupa, Appl. Phys. B **71**, 131 (2000).
[2] S. Im, J. Y. Jeong, M. S. Oh, H. B. Kim, K. H. Chae, C. N. Whang, and J. H. Song, Appl. Phys. Lett. **74**, 961 (1999).
[3] J. M. J. Lopes, F. C. Zawislak, M. Behar, P. F. P. Fichtner, L. Rebohle, and W. Skorupa, J. Appl. Phys. **94**, 6059 (2003).
[4] A. Nakajima, T. Futatsugi, H. Nakao, T. Usuki, N. Horiguchi, and N. Yokoyama, J. Appl. Phys. **84**, 1316 (1998).
[5] T. Müller, K.-H. Heining, and W. Möller, Appl. Phys. Lett. **81**, 3049 (2002).
[6] B. Schmidt, D. Grambole, and F. Herrmann, Nucl. Instrum. Methods Phys. Res. B **191**, 482 (2002).
[7] J. M. J. Lopes, F. C. Zawislak, P. F. P. Fichtner, F. C. Lovey, and A. M. Condó, Appl. Phys. Lett. **86**, 023101 (2005).
[8] *Powder Diffraction File Database Sets 1-45*, International Centre for Diffraction Data (ICCD, PA, 1995), PDF number: 040673.
[9] R. W. Olesinski and G. J. Abbaschian, in *Binary Alloy Phase Diagrams*, 2nd ed., edited by T. B. Massalski (ASM International, Ohio, 1992), p. 3362.
[10] Y. Lei, P. Möck, T. Topuria, N. D. Browning, R. Ragan, K. S. Min, and H. A. Atwater, Appl. Phys. Lett. **82**, 4262 (2003), and references cited therein.
[11] R. E. de Lamaestre, H. Bernas, and F. Jomard, Nucl. Instrum. Methods Phys. Res. B **216**, 402 (2004).
[12] T. Okuno, Y. Masumoto, M. Ikezawa, T. Ogawa, and A. A. Lipovskii, Appl. Phys. Lett. **77**, 504 (2000).